Stereochemical Requirements for β-Hairpin Formation: Model Studies with Four-Residue Peptides and Depsipeptides

Tasir S. Haque, Jennifer C. Little, and Samuel H. Gellman*

Contribution from the Department of Chemistry, University of Wisconsin, Madison, Wisconsin 53706

Received February 9, 1996[⊗]

Abstract: Spectroscopic and crystallographic data are presented for a series of tetrapeptides and analogous depsipeptides that can form a minimal β-hairpin (two intramolecular hydrogen bonds). These model compounds have been used to test the hypothesis that "mirror image" β-turns promote β-hairpin formation. This hypothesis was inspired by a statistical survey of β-hairpins in globular proteins (Sibanda, B. L.; Thornton, J. M. *Nature* **1985**, *316*, 170), which showed that mirror image β-turns (type I′ and type II′), although rare in general, are very commonly associated with β-hairpins containing a two-residue loop between the strand segments. Each of our four-residue molecules contains proline at the second position, to promote a central β-turn. The β-turn is induced to be either "common" or "mirror-image", relative to the outer residues, by choice of residue configuration (L vs D). In methylene chloride, end-capped tetrapeptide Ac−L-Val-D-Pro-D-Ala-L-Leu-NMe_2 folds largely into the β-hairpin conformation, while the diastereomer Ac-L-Val-L-Pro-L-Ala-L-Leu-NMe_2 displays little or no β-hairpin folding. For each diastereomer, the hydrogen-bonded driving force for β-hairpin folding is identical, and the dramatic difference in folding behavior therefore reflects a variation in the intrinsic conformational properties of the diastereomeric backbones. Similar behavior is seen for the diastereomeric peptide pair Ac-L-Val-D-Pro-Gly-L-Leu-NMe_2 vs Ac-L-Val-L-Pro-Gly-L-Leu-NMe_2, and for the analogous depsipeptides with a lactic acid or glycolic acid residue at the third position. Thus, our results show not only that mirror-image Pro-X turns strongly promote β-hairpin folding, but also that common β-turns strongly discourage formation of a β-hairpin with a two-residue loop.

Introduction

The combination of nonbonded forces that controls formation of β-sheets in proteins is not yet well understood. Individual amino acid residues have characteristic propensities to participate in β-sheets, but the relative importance of such intrinsic propensities and of "context" (i.e., nearest neighbors) is still under debate.[1] β-Sheets in proteins often form from discontinuous polypeptide segments, unlike α-helices or β-turns, and this feature may explain why there have been many model studies of α-helix[2] and β-turn[3] stability, but few such studies of β-sheet stability.[1] It is important to identify the most effective strategies for assembling peptide strands into β-sheets, for rationalizing natural protein folding patterns, and for designing new proteins.[4]

The simplest way to bring two antiparallel strands together is a short peptide segment between the C-terminus of one strand and the N-terminus of the other. This strand−loop−strand arrangement, referred to as a "β-hairpin", is often observed in globular proteins.[5,6] The shortest common loop is two residues; in this case, the two loop residues are the second and third residues of a β-turn. In crystalline proteins, two-residue β-hairpin loops display distinctive conformational propensities, as pointed out by Thornton et al.[5] β-Turn conformations are classified by the φ and ψ torsion angles of the middle two of the four residues (i.e., the two residues of the minimal β-hairpin's loop).[3g] The majority of β-turns in folded proteins adopt type I and type II conformations, but these "common" turns are rare in two-residue β-hairpins. Turns that serve as two-residue β-hairpin loops tend to be type I' and type II', where the prime indicates that the φ and ψ torsion angles of the central residues are opposite to those in the corresponding common turns. (Type I' and II' are often called "mirror image" turns, even though these conformations are actually *diastereomerically* related to the type I and II turn conformations, respectively, unless both central residues are glycine.) Sibanda and Thornton rationalized the correlation between mirror image turns and β-hairpins by noting that the natural twist of these rare turns (but not of the common type I and II turns) is compatible with the natural twist between two strands of antiparallel β-sheet formed from L-amino acids.[5b]

When a local conformational trend is observed in a folded protein, it is difficult to know whether this trend results from

⊗ Abstract published in *Advance ACS Abstracts,* July 15, 1996.

(1) (a) Kim, C. A.; Berg, J. M. *Nature* **1993**, *362*. 267. (b) Minor, D. L.; Kim, P. S. *Nature* **1994**, *367*, 660. (c) Minor, D. L.; Kim, P. S. *Nature* **1994**, *371*, 264. (d) Smith, C. K.; Withka, J. M.; Regan, L. *Biochemistry* **1994**, *33*, 5510. (e) Smith, C. K.; Regan, L. *Science* **1995**, *270*, 980.

(2) (a) Wojcik, J.; Altmann, K.-H.; Scheraga, H. A. *Biopolymers* **1990**, *30*, 121. (b) Scholtz, J. M.; Baldwin, R. L. *Annu. Rev. Biophys. Biomol. Struct.* **1992**, *21*, 95. (c) O'Neil, K. T.; DeGrado, W. F. *Science* **1990**, *250*, 646. (d) Lyu, P. G.; Liff, M. I.; Marky, L. A.; Kallenbach, N. R. *Science* **1990**, *250*, 669. (e) Merutka, G.; Lipton, W.; Shalongo, W.; Park, S.-H.; Stellwagen, E. *Biochemistry* **1990**, *29*, 7511. (f) Kemp, D. S.; Boyd, J. G.; Mundel, C. *Nature* **1991**, *352*, 451.

(3) (a) Boussard, G.; Marraud, M. *J. Am. Chem. Soc.* **1985**, *107*, 1825. (b) Wright, P. E.; Dyson, H. J.; Lerner, R. A. *Biochemistry* **1988**, *27*, 7167. (c) Falcomer, C. M.; Meinwald, Y. C.; Choudhary, I.; Talluri, S.; Milburn, P. J.; Clardy, J.; Scherage, H. A. *J. Am. Chem. Soc.* **1992**, *114*, 4036. (d) Liu, X.; Scott, P. G.; Otter, A.; Kotovych, G. *Biopolymers* **1992**, *32*, 119. (e) Pietrzynski, G.; Rzeszotarska, B.; Kubica, Z. *Int. J. Peptide Protein Res.* **1992**, *40*, 524. (f) Liang, G.-B.; Rito, C. J.; Gellman, S. H. *J. Am. Chem. Soc.* **1992**, *114*, 4440. (g) Rose, G. D.; Gierasch, L. M.; Smith, J. A. *Adv. Protein Chem.* **1985**, *37*, 1.

(4) Leading references on β-sheet protein design efforts: (a) Kullmann, W. *J. Med. Chem.* **1984**, *27*, 106. (b) Klauser, S.; Gantner, K.; Salgam, P.; Gutte, B. *Biochem. Biophys. Res. Commun.* **1991**, *179*, 1212. (c) Quinn, T. P.; Tweedy, N. B.; Williams, R. W.; Richardson, J. S.; Richardson, D. C. *Proc. Natl. Acad. Sci. U.S.A.* **1994**, *91*, 8747. (d) Yan, Y.; Erickson, B. W. *Protein Sci.* **1994**, *3*, 1069.

(5) (a) Sibanda, B. L.; Thornton, J. M. *Nature* **1985**, *316*, 170. (b) Wilmot, C. M.; Thornton, J. M. *J. Mol. Biol.* **1988**, *203*, 221. (c) Sibanda, B. L.; Thornton, J. M. *J. Mol. Biol.* **1993**, *229*, 428.

(6) Short peptides folded into β-hairpins under non-aqueous conditions: (a) Ueki, T.; Bando, S.; Ashida, T.; Kakudo, M. *Acta Crystallogr.* **1971**, *B27*, 2219. (b) Karle, I. L.; Kishore, R.; Raghothama, S.; Balaram, P. *J. Am. Chem. Soc.* **1988**, *110*, 1958. (c) Awasthi, S. K.; Raghothama, S.; Balaram, P. *Biochem. Biophys. Res. Commun.* **1995**, *216*, 375.

S0002-7863(96)00429-5 CCC: $12.00

local or nonlocal forces. In order to determine whether the correlation between mirror image turns and two-residue β-hairpin loops reflects an intrinsic conformational preference of peptide backbones, we have examined the folding of tetrapeptides and analogous depsipeptides in solution.[7] A tetrapeptide can adopt a "minimal β-hairpin" conformation, defined by the presence of the 10- and 14-membered ring N−H--O═C hydrogen bonds illustrated below. Selective incorporation of D-residues allows us to predispose the inner two residues to form a "mirror image" turn, relative to the outer two residues. We probe the correlation between intrinsic β-hairpin propensity and the presence of a "mirror image" turn conformation by comparing the folding behavior of all-L molecules and their heterochiral diastereomers.

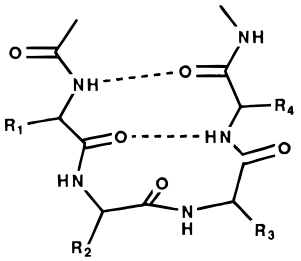

Minimal β-hairpin

In these small molecules, intramolecular hydrogen bonding provides a principal driving force for β-turn and β-hairpin formation. For this reason, many of our studies have been carried out in a relatively nonpolar solvent (methylene chloride), which does not provide strong hydrogen bonding competition. In each diastereomeric comparison discussed below, the hydrogen bonding options are identical between the isomers, but the intrinsic folding propensity of the backbone varies between isomers. Elucidation of these intrinsic folding propensities, which should be largely independent of solvent, is the central goal of these studies.

Our experimental approach requires that the central two residues of the model compounds have a large tendency to adopt β-turn conformations. The presence of L-proline at the second of the four β-turn residues is well-known to promote formation of type I and type II turns,[3g] and all of our compounds contain proline as the second residue. Further predisposition for β-turn formation is achieved in one set of model compounds by using an α-hydroxy acid residue rather than an α-amino acid residue in the third position, which results in an ester rather than an amide linkage between the second and third residues. End-capped Pro-X dipeptides are known to equilibrate between β-turn and γ-turn conformations (the latter involves a seven-membered-ring hydrogen bond across the proline residue) in nonpolar solvents at room temperature,[3f] while the analogous depsipeptides exist almost exclusively in the β-turn conformation (10-membered-ring hydrogen bond; Scheme 1).[8] Crystallographic analysis of Pro-X depsipeptides[8] indicates that the α-hydroxy acid residue is a good structural mimic for an α-amino acid residue, as one would expect in light of the similar conformational properties of secondary amide and ester units.

The experiments below involve four tetrapeptides, containing the sequences Val-Pro-Ala-Leu and Val-Pro-Gly-Leu, and five depsipeptides, with Ala or Gly replaced by lactic acid (Lac) or glycolic acid (Glyco), respectively. The terminal residues were chosen based on their tendencies in proteins to occupy the first and fourth positions of β-turns embedded in hairpins,[5] and with an eye toward maximizing solubility in nonpolar solvents. These molecules are illustrated in Chart 1, along with the shorthand designations used in the text.

Scheme 1

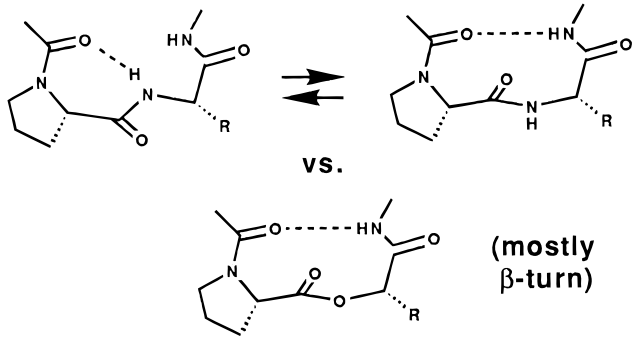

Chart 1

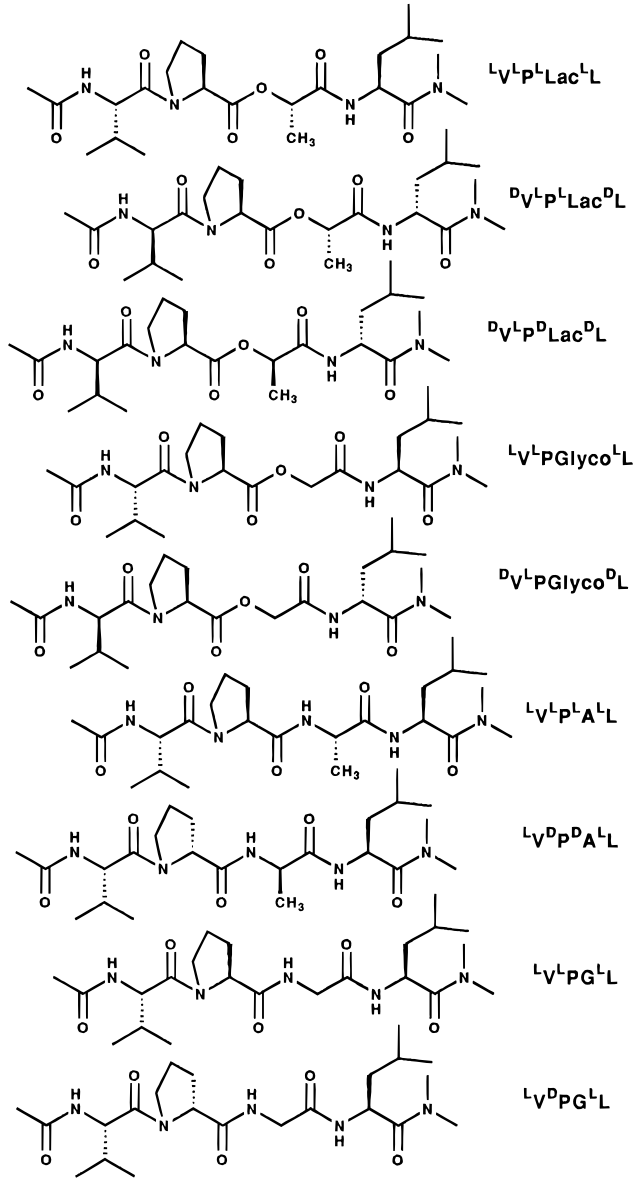

Results and Discussion

Depsipeptides in Methylene Chloride. Figure 1 shows the variation in the amide proton ^{1}H NMR chemical shifts for ^{D}V^{L}PGlyco^{D}L and ^{L}V^{L}PGlyco^{L}L in CD_2Cl_2 as a function of

(7) A preliminary report has appeared on the depsipeptides discussed here: Haque, T. S.; Little, J. C.; Gellman, S. H. *J. Am. Chem. Soc.* **1994**, *116*, 4105.

(8) Boussard, G.; Marraud, M.; Neel, J.; Maigret, M.; Aubry, A. *Biopolymers* **1977**, *16*, 1033.

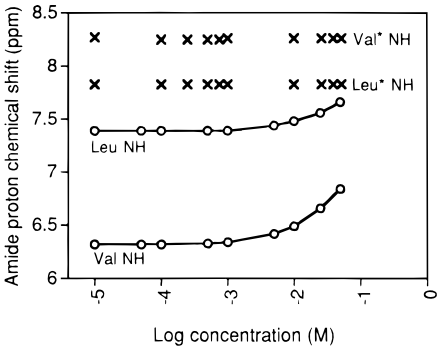

Figure 1. Amide proton NMR chemical shifts in CD_2Cl_2 at room temperature, as a function of the logarithm of depsipeptide concentration: (×) Val NH ("Val* NH") and Leu NH ("Leu* NH") of $^{D}V^{L}PGlyco^{D}L$; (—, ○) Val NH and Leu NH of $^{L}V^{L}PGlyco^{L}L$.

the logarithm of depsipeptide concentration. In order to facilitate interpretation of this graph, we display the behavior of the all-L depsipeptide with continuous lines, while the data for $^{D}V^{L}PGlyco^{D}L$ are shown with symbols. The chemical shift of an amide proton is usually very sensitive to hydrogen bonding, and these data, spanning more than three orders of magnitude in concentration, provide insight on the concentrations at which aggregation (i.e., intermolecular hydrogen bonding) occurs. Both amide protons of the all-L isomer shift downfield above ca. 5 mM, indicating the onset of aggregation at this concentration. In contrast, neither amide proton of $^{D}V^{L}PGlyco^{D}L$ displays any concentration dependence, which suggests that this depsipeptide does not aggregate in the concentration range examined. An alternative possibility, that $^{D}V^{L}PGlyco^{D}L$ is fully aggregated at 0.01 mM, seems exceedingly unlikely, given that each molecule contains just two hydrogen bond donor sites.

For a given amide proton, increased population of hydrogen bonded states leads to a downfield shift (hydrogen bonding equilibration in flexible molecules is rapid on the NMR time scale, and the observed δNH reflects a population-weighted average of contributing hydrogen bonded and non-hydrogen bonded states). Comparisons between analogous protons in diastereomers therefore provide insight on the extent of hydrogen bonding at the amide proton in question. The behavior of the valine NH is of particular interest, since this proton can participate in the 14-membered-ring hydrogen bond that defines the minimal β-hairpin (involving the leucine C═O). For $^{D}V^{L}PGlyco^{D}L$, Val NH appears at 8.25 ppm, while for the all-L isomer, Val NH appears at 6.35 ppm, in the concentration-independent limit. The latter chemical shift is characteristic of a peptide backbone proton that experiences little or no hydrogen bonding in CD_2Cl_2, while the former chemical shift indicates a large amount of intramolecular hydrogen bonding.[3f,9] In contrast to the 1.9-ppm separation between the Val NH's, the Leu NH's of these diastereomers are only 0.4 ppm apart, which is consistent with there being a substantial population of the β-turn folding pattern (10-membered-ring hydrogen bond) in both molecules. Thus, the δNH comparison between $^{L}V^{L}PGlyco^{L}L$ and $^{D}V^{L}PGlyco^{D}L$ suggests that the all-L isomer experiences significant β-turn folding, but little or no β-hairpin folding, while the diastereomer in which the inner residues are predisposed to form a mirror image turn, relative to the outer (Val and Leu) residues, is largely folded into the β-hairpin. The analogous ^{1}H NMR data previously reported[7] for $^{L}V^{L}P^{L}Lac^{L}L$ and $^{D}V^{L}P^{L}Lac^{D}L$ imply a similar pattern of folding behavior for this diastereomeric pair. These conformational deductions are summarized in Scheme 2.

Figure 2 shows FT-IR data from the N−H stretch region for all five depsipeptides, $^{L}V^{L}P^{L}Lac^{L}L$, $^{D}V^{L}P^{L}Lac^{D}L$, $^{L}V^{L}PGlyco^{L}L$, $^{D}V^{L}PGlyco^{D}L$, and $^{D}V^{L}P^{D}Lac^{D}L$ in CH_2Cl_2 (each depsipeptide 1 mM, i.e., below the onset of aggregation). We have previously made extensive use of N−H stretch data obtained in dilute CH_2Cl_2 solution to analyze intramolecular hydrogen bonding in peptides, depsipeptides, and related molecules.[9] These prior studies allow straightforward interpretation of the data in Figure 2. For both all-L depsipeptides, two bands of similar intensity are observed, at 3422 and ca. 3310 cm^{-1}. The former results from a weak intraresidue five-membered ring N−H--O═C interaction ("C_5 interaction"; whether or not this interaction constitutes a hydrogen bond has been a subject of debate).[10] The bands near 3310 cm^{-1} arise from N−H involved in typical amide-to-amide hydrogen bonds. Thus, a substantial proportion of the N−H in the all-L depsipeptides is free of interresidue hydrogen bonding, which is consistent with our hypothesis (Scheme 2) that these depsipeptides experience considerable β-turn formation but little or no β-hairpin formation. The heterochiral depsipeptides $^{D}V^{L}P^{L}Lac^{D}L$ and $^{D}V^{L}PGlyco^{D}L$, however, display only one N−H stretch band, at ca. 3296 cm^{-1}, which is consistent with formation of strong intramolecular amide-to-amide hydrogen bonds. The absence of a band between 3400 and 3500 cm^{-1} for these depsipeptides indicates that both amide protons are fully hydrogen bonded, i.e., that the β-hairpin conformations are fully populated under these conditions (Scheme 2). (For these molecules, only the β-hairpin folding pattern allows formation of two strong intramolecular amide-to-amide hydrogen bonds simultaneously.)

It has long been known that placement of a D-residue at the third position of an otherwise all-L β-turn promotes formation of a type II turn, and that L-Pro-D-Xxx sequences are particularly strong type II turn inducers.[11] We therefore examined $^{D}V^{L}P^{D}Lac^{D}L$, the central two residues of which should form a mirror image turn relative to the outer residues. The rightmost spectrum in Figure 2 shows N−H stretch region IR data for a 1 mM solution of this depsipeptide in CH_2Cl_2. The major band occurs at 3308 cm^{-1}, in the region for strong amide-to-amide hydrogen bonds. Unlike the other two heterochiral depsipeptides, however, there is also a tiny absorbance at 3420 cm^{-1}. Thus, the mirror image turn strongly promotes β-hairpin formation in $^{D}V^{L}P^{D}Lac^{D}L$, although not quite to the extent observed for $^{D}V^{L}P^{L}Lac^{D}L$ and $^{D}V^{L}PGlyco^{D}L$.

Long-range nuclear Overhauser effects, detected via a ROESY experiment,[12] provided further evidence of β-hairpin folding for $^{D}V^{L}P^{L}Lac^{D}L$, $^{D}V^{L}PGlyco^{D}L$, and $^{D}V^{L}P^{D}Lac^{D}L$ in CD_2Cl_2. This folding pattern requires that the two amide protons lie near one another in space, and the expected Val NH--Leu NH cross peak was observed for all three heterochiral depsipeptides (Figure 3). No such cross peak was observed in ROESY spectra of the all-L depsipeptides. It should be noted that an NOE between protons that are so covalently distant from one another is more strongly diagnostic of a compact conformation than are NOEs between protons on adjacent residues (the latter are commonly adduced to support population of β-turns and other secondary structures in short peptides). NH--NH cross peaks between adjacent residues, for example, are consistent with β-turn and α-helix conformations, but as Landis et al. have recently shown,[13] such relatively short-range interactions can also arise from other conformations available to flexible peptides.

(9) (a) Dado, G. P.; Gellman, S. H. *J. Am. Chem. Soc.* **1993**, *115*, 4228. (b) Gallo, E. A.; Gellman, S. H. *J. Am. Chem. Soc.* **1993**, *115*, 9774. (c) Gallo, E. A.; Gellman, S. H. *J. Am. Chem. Soc.* **1994**, *116*, 11560.

(10) (a) Avignon, M.; Huong, P. V.; Lascombe, J.; Marraud, M.; Neel, J. *Biopolymers* **1969**, *8*, 69. (b) Burgess, A. W.; Scheraga, H. A. *Biopolymers* **1973**, *12*, 2177.

(11) Boussard, G.; Marraud, M.; Néel, J. *J. Chim. Phys.* **1974**, *71*, 1081.

(12) Bothner-By, A. A.; Stephens, R. L.; Lee, J.; Warren, C. D.; Jeanloz, R. W. *J. Am. Chem. Soc.* **1984**, *106*, 811.

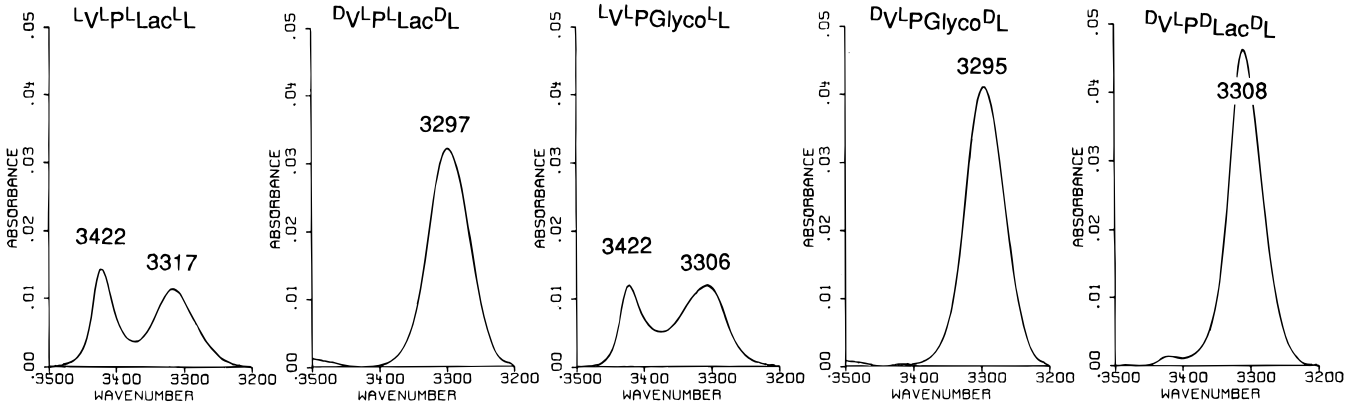

Figure 2. N−H stretch FT-IR data for 1 mM depsipeptide samples in CH_2Cl_2 at room temperature, after subtraction of the spectrum of pure CH_2Cl_2. From left to right: $^{L}V^{L}P^{L}Lac^{L}L$, maxima at 3422 and 3317 cm^{-1}; $^{D}V^{L}P^{L}Lac^{D}L$, maximum at 3297 cm^{-1}; $^{L}V^{L}PGlyco^{L}L$, maxima at 3422 and 3306 cm^{-1}; $^{D}V^{L}PGlyco^{D}L$, maximum at 3295 cm^{-1}; $^{D}V^{L}P^{D}Lac^{D}L$, maxima at 3420 and 3308 cm^{-1}.

Scheme 2. Major Folding Patterns of Depsipeptides in Methylene Chloride and Acetonitrile

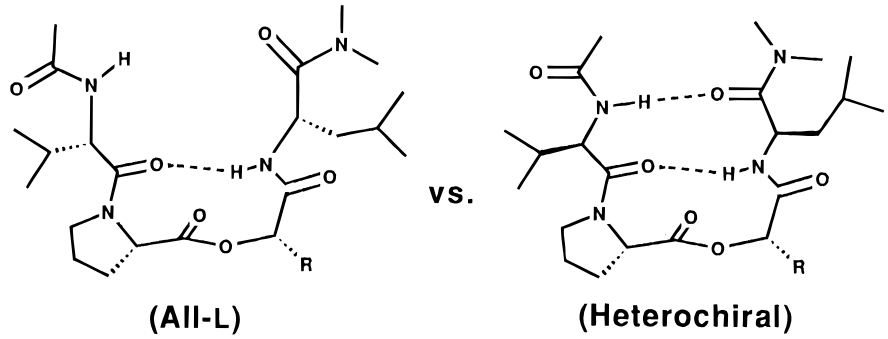

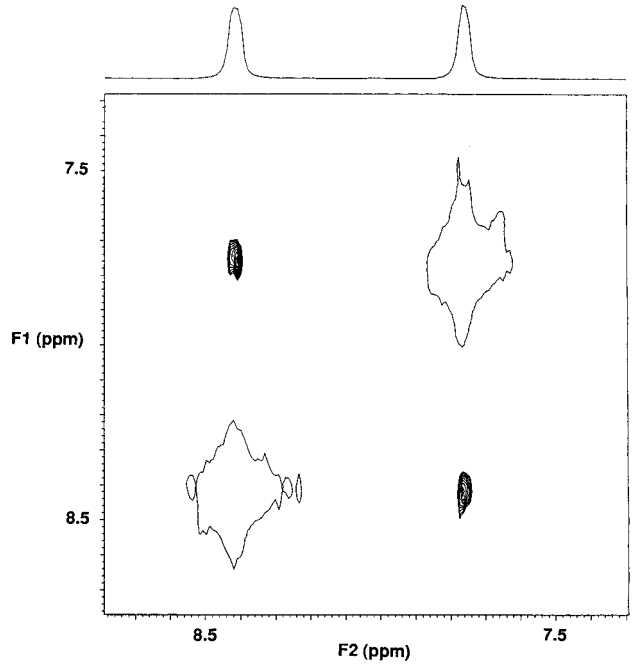

Figure 3. The amide proton portion of the 500-MHz ROESY spectrum of depsipeptide $^{D}V^{L}P^{L}Lac^{D}L$, 1 mM in CD_2Cl_2 at 297 K. Data were acquired on a Varian Unity instrument using the ROESY pulse sequence that is part of the standard Varian software, with 2048 data points along t_2, 128 t_1 increments, and 112 scans per t_1 increment. The mixing time was 0.50 s, accompanied by a relaxation delay of 1.20 s and a "homospoil" relaxation pulse. The spectral width was 6000 Hz. Additional details may be found in the Experimental Section. Proton assignments were made on the basis of TOCSY data.

Depsipeptides in Acetonitrile and DMSO. These two solvents provide an increase in hydrogen bonding competition relative to methylene chloride: acetonitrile is a modest hydrogen bond acceptor, and DMSO is a strong acceptor. N−H stretch region IR data for $^{L}V^{L}P^{L}Lac^{L}L$, $^{D}V^{L}P^{L}Lac^{D}L$, $^{L}V^{L}PGlyco^{L}L$, and $^{D}V^{L}PGlyco^{D}L$ in CH_3CN (Figure 4) show that folding behavior in this solvent is similar to that observed in CH_2Cl_2. (CH_3CN IR data were obtained with 10 mM solutions; we assume that there is no aggregation under these conditions, by extrapolation from the methylene chloride results.) Each of the all-L depsipeptides displays two maxima in the N−H stretch region, at ca. 3370 and 3310 cm^{-1}. The lower energy bands are very similar in position to those observed for the same molecules in CH_2Cl_2, and we attribute these bands to N−H moieties engaged in intramolecular amide-to-amide hydrogen bonds (presumably the 10-membered-ring β-turn hydrogen bond). The higher energy bands are ca. 50 cm^{-1} lower than the analogous bands in CH_2Cl_2; these bands in Figure 4 are assigned to N−H groups interacting with CH_3CN. (Solvent-exposed amide groups in CH_3CN display an N−H stretch band that is 50−60 cm^{-1} lower in energy than the corresponding band in CH_2Cl_2;[14] this solvent-induced shift presumably results from weak CH_3CN--H−N hydrogen bonds.) Thus, there appears to be considerable β-turn but little or no β-hairpin for the all-L depsipeptides in CH_3CN, as was observed in CH_2Cl_2.

The IR data for heterochiral depsipeptides $^{D}V^{L}P^{L}Lac^{D}L$ and $^{D}V^{L}PGlyco^{D}L$ in CH_3CN (Figure 4) are nearly identical to the data obtained in CH_2Cl_2 (Figure 2), indicating that the β-hairpin induced by a mirror image turn is sufficiently robust to resist hydrogen bond competition from surrounding CH_3CN molecules. (We have previously observed that CH_3CN can disrupt less stable intramolecular hydrogen bonding patterns.[14]) The population of β-hairpin conformations by the heterochiral depsipeptides in acetonitrile is supported by ROESY data: the hairpin-characteristic Val NH--Leu NH cross peak is observed for both $^{D}V^{L}P^{L}Lac^{D}L$ and $^{D}V^{L}PGlyco^{D}L$, although the intensity

(13) Landis, C. R.; Luck, L. L.; Wright, J. M. *J. Magn. Reson. B* **1995**, *109*, 44.

(14) Gellman, S. H.; Dado, G. P.; Liang, G.-B.; Adams, B. R. *J. Am. Chem. Soc.* **1991**, *113*, 1164.

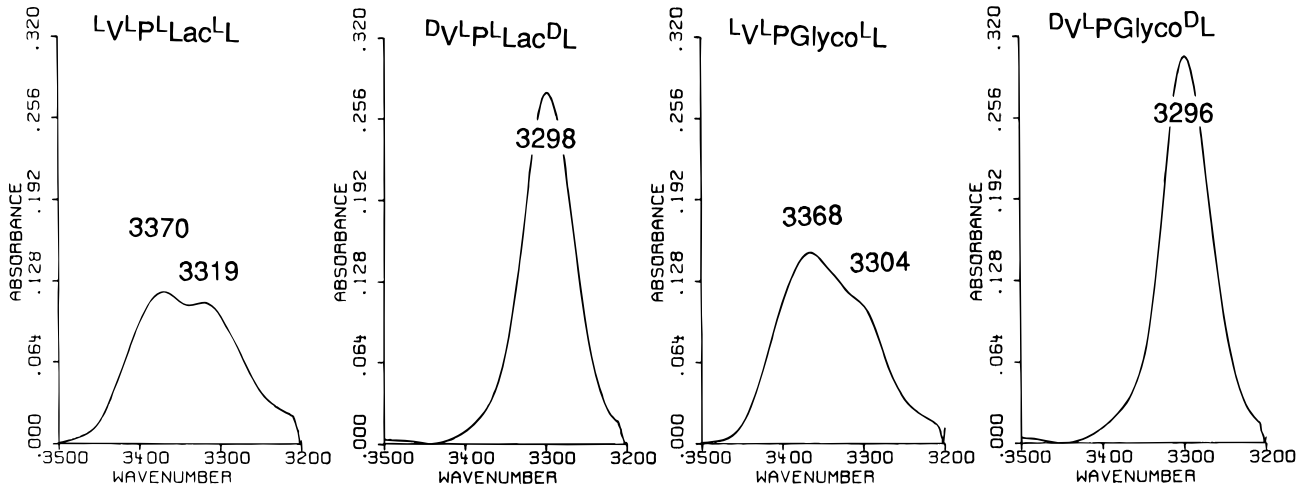

Figure 4. N−H stretch FT-IR data for 10 mM depsipeptide samples in CH_3CN at room temperature, after subtraction of the spectrum of pure CH_3CN. From left to right: $^{L}V^{L}P^{L}Lac^{L}L$, maxima at 3370 and 3319 cm^{-1}; $^{D}V^{L}P^{L}Lac^{D}L$, maximum at 3298 cm^{-1}; $^{L}V^{L}PGlyco^{L}L$, maxima at 3368 and 3304 cm^{-1}; $^{D}V^{L}PGlyco^{D}L$, maximum at 3296 cm^{-1}.

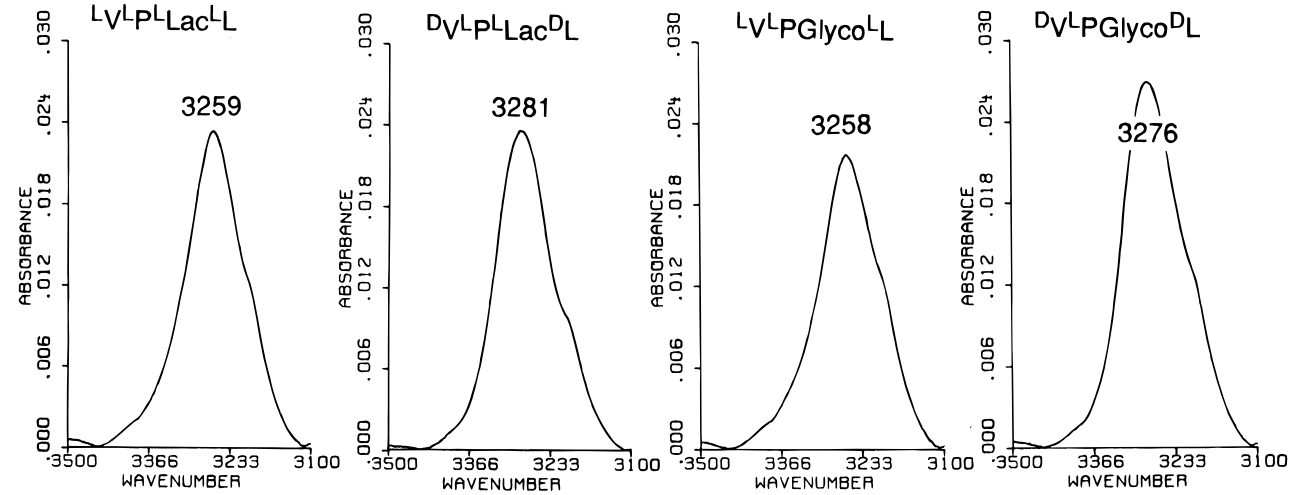

Figure 5. N−H stretch FT−IR data for 10 mM depsipeptide samples in DMSO at room temperature, after subtraction of the spectrum of pure DMSO. From left to right: $^{L}V^{L}P^{L}Lac^{L}L$, maximum at 3259 cm^{-1}; $^{D}V^{L}P^{L}Lac^{D}L$, maximum at 3281 cm^{-1}; $^{L}V^{L}PGlyco^{L}L$, maximum at 3258 cm^{-1}; $^{D}V^{L}PGlyco^{D}L$, maximum at 3276 cm^{-1}.

is weaker for the latter. A weak NH--NH cross peak is observed also for $^{D}V^{L}P^{D}Lac^{D}L$ in CD_3CN, but not for the all-L depsipeptides.

DMSO IR data for $^{L}V^{L}P^{L}Lac^{L}L$, $^{D}V^{L}P^{L}Lac^{D}L$, $^{L}V^{L}PGlyco^{L}L$, and $^{D}V^{L}PGlyco^{D}L$ are shown in Figure 5. N−H stretch signals lose their diagnostic spectral dispersion in this solvent, because amide-to-DMSO hydrogen bonds and strong amide-to-amide hydrogen bonds give rise to bands in the same region of the IR spectrum. Nevertheless, an interesting pattern is observed among the data in Figure 5: the all-L depsipeptides display a maximum at 3258 cm^{-1}, while the maxima for $^{D}V^{L}P^{L}Lac^{D}L$ and $^{D}V^{L}PGlyco^{D}L$ are ca. 20 cm^{-1} higher in wavenumber. The CH_2Cl_2 and CH_3CN data show that amide-to-amide hydrogen bonded N−H occurs in the range 3290−3300 cm^{-1}. Therefore, the difference between the all-L depsipeptides and their heterochiral isomers in DMSO suggests that significant β-hairpin folding is retained by $^{D}V^{L}P^{L}Lac^{D}L$ and $^{D}V^{L}PGlyco^{D}L$ in this solvent, while the all-L isomers are largely unfolded and hydrogen bonded to DMSO. A weak ROESY Val NH--Leu NH cross peak was observed for $^{D}V^{L}P^{L}Lac^{D}L$ in DMSO-d_6, which is good evidence for the existence of some β-hairpin structure in this very competitive solvent. No NH--NH cross peak was detected for $^{D}V^{L}PGlyco^{D}L$ or $^{D}V^{L}P^{D}Lac^{D}L$ in DMSO-d_6.

Cis/Trans Proline Rotamer Ratios. Adoption of a β-turn or β-hairpin conformation by our four-residue molecules requires that the proline exist as the *trans* rotamer. Table 1 shows the *cis:trans* ratios for the depsipeptides $^{L}V^{L}P^{L}Lac^{L}L$, $^{D}V^{L}P^{L}Lac^{D}L$, $^{L}V^{L}PGlyco^{L}L$, and $^{D}V^{L}PGlyco^{D}L$ in the three solvents employed in these studies. The ratios in methylene chloride and acetonitrile are consistent with our contention that the heterochiral sequences promote β-hairpin formation, but these data do not in themselves constitute strong evidence for this deduction, since the amount of *cis* proline is always low. Greater amounts of *cis* proline are observed in DMSO than in the other two solvents, which is consistent with the general trend that increasing solvent polarity favors the *cis* form.[15] Interestingly, the all-L molecules show lower *cis:trans* ratios than the heterochiral molecules in DMSO. The origin of this trend is unclear, but the *cis:trans* ratio cannot be related to β-hairpin formation in DMSO, since we have independent evidence for some population of β-hairpin

Table 1. *Cis:Trans* Ratios

depsipeptide	CD_2Cl_2	CD_3CN	DMSO-d_6
$^{L}V^{L}P^{L}Lac^{L}L$	6:94	7:93	4:96
$^{D}V^{L}P^{L}Lac^{D}L$	*a*	*a*	12:87
$^{L}V^{L}PGlyco^{L}L$	*a*	5:95	5:95
$^{D}V^{L}PGlyco^{D}L$	*a*	*a*	15:85
$^{D}V^{L}P^{D}Lac^{D}L$	*a*	3:97	25:75

[a] Cis rotamer not detected.

(15) Higashijima, T.; Tasumi, M.; Miyazawa, T. *Biopolymers* **1977**, *16*, 1259.

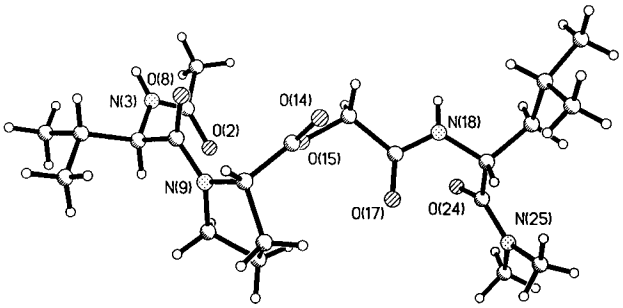

Figure 6. Ball-and-stick representation of the solid state conformation of $^{D}V^{L}PGlyco^{D}L$, as determined by X-ray diffraction. The two amide protons are engaged in intermolecular hydrogen bonds (not shown). Numbering is given for nitrogen and oxygen atoms only.

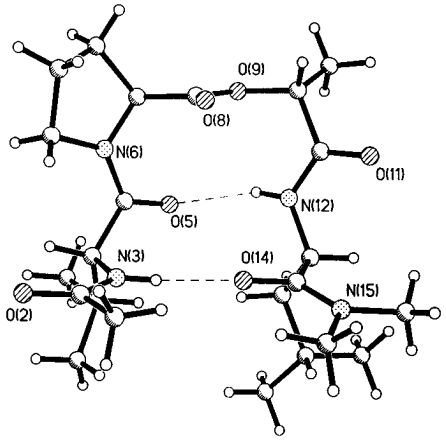

Figure 7. Ball-and-stick representation of the solid state conformation of $^{D}V^{L}P^{D}Lac^{D}L$, as determined by X-ray diffraction. The two intramolecular hydrogen bonds are indicated by dashed lines. Numbering is given for nitrogen and oxygen atoms only.

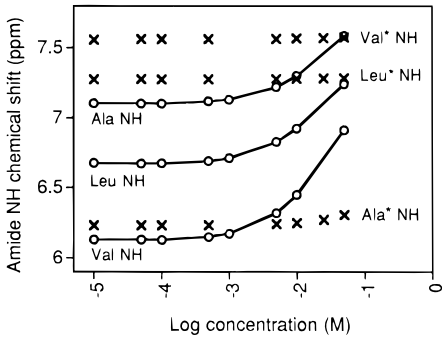

Figure 8. Amide proton NMR chemical shifts in CD_2Cl_2 at room temperature, as a function of the logarithm of peptide concentration: (×) Val NH ("Val* NH"), Leu NH ("Leu* NH"), and Ala NH ("Ala* NH") of $^{L}V^{D}P^{D}A^{L}L$; (—, ○) to Val NH, Leu NH, and Ala NH of $^{L}V^{L}P^{L}A^{L}L$.

conformations for heterochiral but not all-L depsipeptides (ROESY data for $^{D}V^{L}P^{L}Lac^{D}L$ and IR data for $^{D}V^{L}P^{L}Lac^{D}L$ and $^{D}V^{L}PGlyco^{D}L$).

Depsipeptide Crystal Structures. Crystals suitable for X-ray diffraction were obtained for both all-L depsipeptides and for $^{D}V^{L}PGlyco^{D}L$ and $^{D}V^{L}P^{D}Lac^{D}L$. The two all-L depsipeptides and $^{D}V^{L}PGlyco^{D}L$ crystallized in extended conformations, with only intermolecular hydrogen bonds formed in the solid state (the solid state conformation of $^{D}V^{L}PGlyco^{D}L$ is shown in Figure 6). $^{D}V^{L}P^{D}Lac^{D}L$, however, crystallized in a β-hairpin conformation, as shown in Figure 7 (L-Pro-D-Lac ϕ and ψ angles, sequentially: −65.0°, 125.2°, 76.8°, 14.5°; these torsion angles correspond to the expected type II turn[3g]).

Tetrapeptides in Methylene Chloride. Figure 8 shows the variation in the amide proton ^{1}H NMR chemical shifts for $^{L}V^{D}P^{D}A^{L}L$ and $^{L}V^{L}P^{L}A^{L}L$ in CD_2Cl_2 as a function of the logarithm of peptide concentration. The all-L peptide aggregates above ca. 1 mM, while $^{L}V^{D}P^{D}A^{L}L$ does not appear to aggregate significantly between 0.01 and 50 mM. Val NH of $^{L}V^{D}P^{D}A^{L}L$, which would be involved in the hairpin-diagnostic 14-membered-ring hydrogen bond, is the furthest downfield of the six amide protons, in the concentration-independent limit. This observation suggests that there is substantial population of the β-hairpin conformation by $^{L}V^{D}P^{D}A^{L}L$. In contrast, Val NH of the all-L isomer is the most upfield of the six amide protons, which implies that there is little or no β-hairpin folding in this case.

As required for β-hairpin formation, Ala NH of $^{L}V^{D}P^{D}A^{L}L$ is quite far upfield, consistent with there being little or no internal hydrogen bonding to this amide proton. Ala NH of the all-L isomer, on the other hand, is the most downfield of this peptide's amide protons, in the concentration-independent limit, suggesting significant hydrogen bonding at this position. The Ala NH chemical shift of the all-L isomer is similar to that observed for the dipeptide Ac-L-Pro-L-Ala-NHMe under identical conditions.[3f] There is a significant population of the γ-turn folding pattern across the proline residue for this dipeptide in methylene chloride at room temperature[3f] (seven-membered-ring hydrogen bond involving the Ala NH; see Scheme 1). Thus, the L-Pro-L-Ala segment of $^{L}V^{L}P^{L}A^{L}L$ apparently exhibits behavior similar to that observed for the isolated dipeptide. Scheme 3 summarizes the conformational behavior we ascribe to $^{L}V^{L}P^{L}A^{L}L$ and $^{L}V^{D}P^{D}A^{L}L$ in methylene chloride; this hypothesis is supported by additional data outlined below, and applies to the glycine-containing tetrapeptides, as well.

Concentration-dependent δNH data for $^{L}V^{L}PG^{L}L$ and $^{L}V^{D}PG^{L}L$ in CD_2Cl_2 are shown in Figure 9. The Val NH chemical shifts (concentration-independent limit) are diagnostic of β-hairpin formation, and in this feature the glycine-containing peptides parallel the alanine-containing peptides. For the all-L isomer, Val NH is far upfield, in the range typical of non-hydrogen bonded peptide NH groups, but for $^{L}V^{D}PG^{L}L$, Val NH is far downfield. There are some differences between the data sets in Figures 8 and 9, however. First, $^{L}V^{D}PG^{L}L$ is more prone to aggregate than $^{L}V^{D}P^{D}A^{L}L$. Second, in the concentration-independent limits, Leu NH is further downfield than Gly NH for $^{L}V^{L}PG^{L}L$, while Leu NH was upfield of Ala NH for $^{L}V^{L}P^{L}A^{L}L$. This latter difference presumably results from the fact that, in the competition between β- and γ-turn folding patterns, the β-turn is relatively more favorable for Ac-L-Pro-Gly-NHMe than for Ac-L-Pro-L-Ala-NHMe.[3f] Thus, the data in Figure 9 suggest that the conformational hypothesis outlined in Scheme 3 applies to $^{L}V^{L}PG^{L}L$ and $^{L}V^{D}PG^{L}L$, but that the position of the β- vs γ-turn equilibrium varies between $^{L}V^{L}P^{L}A^{L}L$ and $^{L}V^{L}PG^{L}L$.

N−H stretch region IR data for $^{L}V^{L}P^{L}A^{L}L$, $^{L}V^{D}P^{D}A^{L}L$, $^{L}V^{L}PG^{L}L$, and $^{L}V^{D}PG^{L}L$ (Figure 10) support the conclusion that the all-L tetrapeptides experience little or no β-hairpin formation, while $^{L}V^{D}P^{D}A^{L}L$ and $^{L}V^{D}PG^{L}L$ are largely folded into the β-hairpin conformation (Scheme 3). For each of the all-L peptides, the major band appears at ca. 3420 cm^{-1}, which, as discussed above, indicates an absence of strong amide-to-amide hydrogen bonding. These peptides display only small or moderate bands in the strong intramolecular hydrogen bonding region (3323 and 3311 cm^{-1}). In contrast, the major bands for $^{L}V^{D}P^{D}A^{L}L$ and $^{L}V^{D}PG^{L}L$ fall in the region that is characteristic of strong intramolecular amide-to-amide hydrogen bonding. Both of these heterochiral peptides have a minor band at higher wavenumber, 3420 cm^{-1} for $^{L}V^{D}P^{D}A^{L}L$ and 3435 cm^{-1} for $^{L}V^{D}PG^{L}L$. If hairpin folding is dominant in these heterochiral molecules, then the Ala or Gly NH should not engage in

Scheme 3. Major Folding Patterns for Tetrapeptides in Methylene Chloride and Acetonitrile

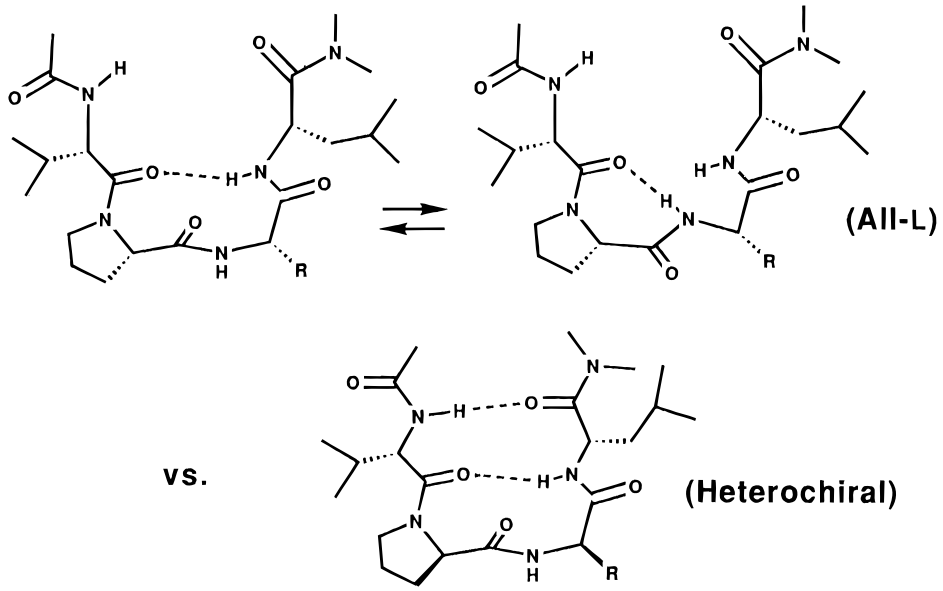

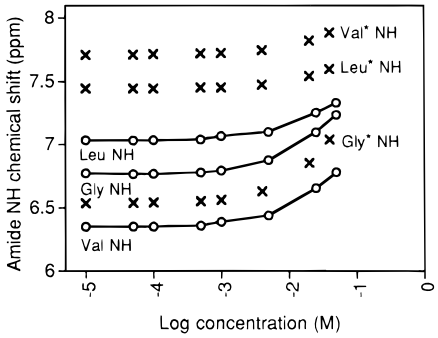

Figure 9. Amide proton NMR chemical shifts in CD_2Cl_2 at room temperature, as a function of the logarithm of peptide concentration: (×) Val NH ("Val* NH"), Leu NH ("Leu* NH"), and Gly NH ("Gly* NH") of $^{L}V^{D}PG^{L}L$; (—, ○) Val NH, Leu NH and Gly NH of $^{L}V^{L}PG^{L}L$.

hydrogen bonding, which would explain the origin of these minor bands. In order to elucidate the origin of the 3420-cm^{-1} band of $^{L}V^{D}P^{D}A^{L}L$, we prepared a version containing ^{15}N-labeled alanine, $^{D}V^{L}P(^{15}N)^{L}A^{D}L$. As expected, the isotopic substitution caused by 3420-cm^{-1} maximum to shift to lower energy[16] (3412 cm^{-1}; rightmost spectrum in Figure 10), but this shift revealed a small shoulder at 3432 cm^{-1}, which we attribute to a small amount of non-hydrogen bonded Val and/or Leu N−H.

NOESY[17] data obtained in CD_2Cl_2 support our deduction that $^{L}V^{D}P^{D}A^{L}L$ and $^{L}V^{D}PG^{L}L$ are folded into β-hairpin conformations to large extents, while the all-L isomers are not (Scheme 3). For both $^{L}V^{D}P^{D}A^{L}L$ and $^{L}V^{D}PG^{L}L$, a long-range Val NH--Leu NH cross peak was observed, as was an additional long-range cross peak between C-terminal and N-terminal methyl groups. The buildup of the long-range cross peaks is shown in Figures 11 and 12, along with the buildup of closer protons, Ala NH--Leu NH and Gly NH--Leu NH, respectively. Although the long-range signals are relatively weak, the data in Figures 11 and 12 indicate that these cross peaks do not result from transferred NOE effects. These long-range cross peaks are not observed for the all-L peptides in CD_2Cl_2. The all-L peptides did display an NOE cross peak between the amide protons of the third and fourth residues (Ala NH--Leu NH or Gly NH--Leu NH), which is conventionally interpreted to indicate the presence of β-turn conformations. As mentioned above, however, this relatively short-range interaction can arise from other types of conformations as well.[13]

Tetrapeptides in Acetonitrile and DMSO. N−H stretch region IR data for $^{L}V^{L}P^{L}A^{L}L$, $^{L}V^{D}P^{D}A^{L}L$, $^{L}V^{L}PG^{L}L$, and $^{L}V^{D}PG^{L}L$ in CH_3CN (Figure 13) imply considerable population of β-hairpin conformations for the heterochiral peptides, but little internal hydrogen bonding for the all-L isomers (Scheme 3). For the all-L peptides, the absorbance maximum appears at ca. 3370 cm^{-1}, characteristic of solvent-exposed NH moieties in CH_3CN. $^{L}V^{L}PG^{L}L$ displays a shoulder at ca. 3300 cm^{-1}, indicating a small population of conformations containing strong intramolecular amide-to-amide hydrogen bonds (given the band widths, one cannot rule out the presence of a small population of such hydrogen bonds in $^{L}V^{L}P^{L}A^{L}L$). For each of the heterochiral peptides, the absorbance maximum falls in the region attributable to NH involved in strong amide-to-amide hydrogen bonds; the maxima are nearly identical to those observed in CH_2Cl_2 (Figure 10). $^{L}V^{D}PG^{L}L$ also displays a shoulder in the region for solvent-exposed NH in CH_3CN, and the breadth of the band for $^{L}V^{D}P^{D}A^{L}L$ suggests that this peptide displays significant absorbance in the solvent-exposed region, too. (For these peptides, β-hairpin formation requires that one of the three NH groups be solvent exposed.)

N−H stretch region data for $^{L}V^{L}P^{L}A^{L}L$, $^{L}V^{D}P^{D}A^{L}L$, $^{L}V^{L}PG^{L}L$, and $^{L}V^{D}PG^{L}L$ in DMSO are shown in Figure 14. For three of the four molecules, the maximum occurs at ca. 3267 cm^{-1}, which is similar to the position of the N−H stretch bands observed for the all-L depsipeptides in DMSO (Figure 5). $^{L}V^{D}PG^{L}L$, however, shows a maximum at 3286 cm^{-1}, which is similar to that observed for the heterochiral depsipeptides in DMSO. Thus, the $^{L}V^{D}PG^{L}L$ data suggest that there may be some β-hairpin folding even in the face of strong hydrogen bonding competition from the solvent. No long-range interactions were detected in NOESY spectra acquired for the tetrapeptides in DMSO-d_6.

(16) For a localized A−B stretch, the band position can be estimated from the equation

$$\nu = (2\pi c)^{-1}\,[k(M_A + M_B)/M_A M_B]^{1/2}$$

where c is the speed of light, k is the force constant of the A−B bond, M_A is the mass of atom A, and M_B is the mass of atom B. (Silverstein, R. M.; Bassler, G. C.; Morrill, T. C. *Spectrometric Identification of Organic Compounds*, 5th ed.; John Wiley & Sons: New York, 1991; p 93.) This calculation predicts a localized ^{15}N−H stretch to be ca. 12 cm^{-1} lower in energy than a ^{14}N−H stretch.

(17) Macura, S.; Ernst, R. R. *Mol. Phys.* **1980**, *41*, 95.

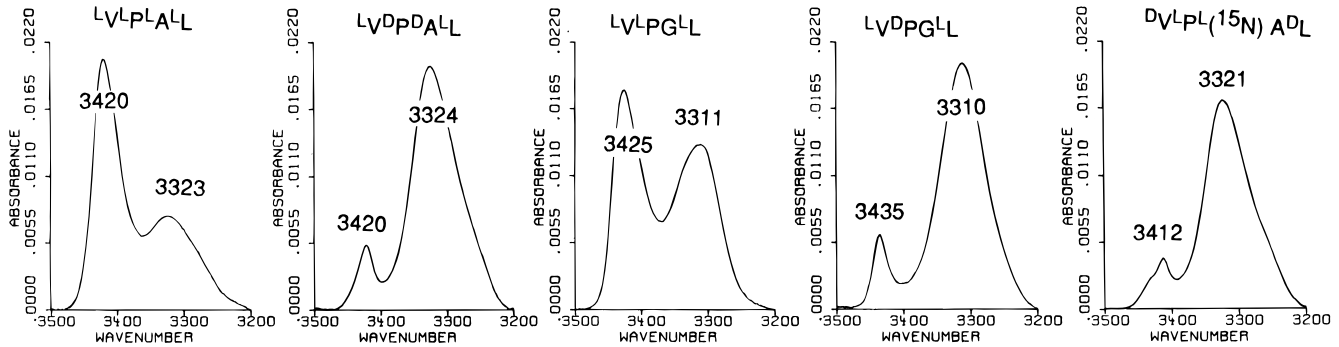

Figure 10. N−H stretch FT-IR data for 1 mM peptide samples in CH_2Cl_2 at room temperature, after subtraction of the spectrum of pure CH_2Cl_2. From left to right: $^{L}V^{L}P^{L}A^{L}L$, maxima at 3420 and 3323 cm^{-1}; $^{L}V^{D}P^{D}A^{L}L$, maxima at 3420 and 3324 cm^{-1}; $^{L}V^{L}PG^{L}L$, maxima at 3425 and 3311 cm^{-1}; $^{L}V^{D}PG^{L}L$, maxima at 3435 and 3310 cm^{-1}; $^{D}V^{L}P^{L}(^{15}N)A^{D}L$, shoulder at 3432 cm^{-1} and maxima at 3412 and 3321 cm^{-1}.

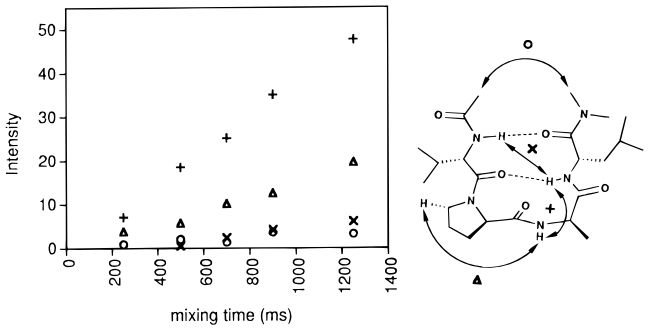

Figure 11. Intensities of selected $^1H-^1H$ NOESY cross peaks as a function of mixing time for a 1 mM sample of $^{L}V^{D}P^{D}A^{L}L$ in CD_2Cl_2. Intensity is in arbitrary units, and is normalized between experiments. Further details may be found in the Experimental Section.

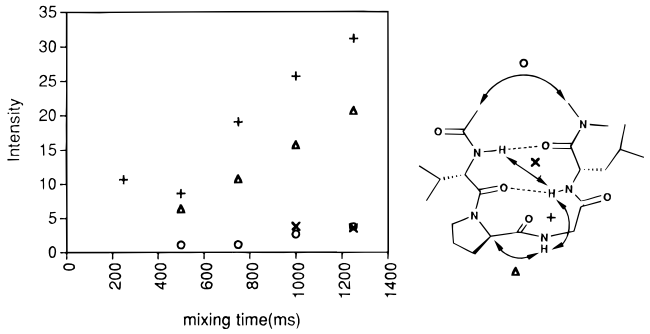

Figure 12. Intensities of selected $^1H-^1H$ NOESY cross peaks as a function of mixing time for a 1 mM sample of $^{L}V^{D}PG^{L}L$ in CD_2Cl_2. Intensity is in arbitrary units, and is normalized between experiments. Further details may be found in the Experimental Section.

Conclusions

1. Mirror-Image *β*-Turns Stabilize Two-Residue Loop *β*-Hairpins. Determining the intramolecular hydrogen bonding pattern is most straightforward in methylene chloride, among the solvents we have examined, and the intramolecular hydrogen bonding pattern identifies the backbone fold. Internal hydrogen bonding information obtained via IR and NMR shows that the heterochiral peptides and depsipeptides are completely or almost completely folded into β-hairpins in methylene chloride, while the all-L isomers experience little or no β-hairpin folding (Schemes 2 and 3). These conclusions are strongly supported by observation of long-range NOE enhancements for the heterochiral peptides and depsipeptides, but not for their all-L analogues. The minimal β-hairpins stabilized by mirror-image turns persist, at least partially, even when hydrogen bonding competition from the solvent undercuts the driving force for folding. Thus, the stabilization of two-residue loop β-hairpins by mirror-image β-turns appears to be quite significant energetically, and our results suggest that selective incorporation of D-residues will prove to be useful for de novo design of β-sheet proteins.[18]

Since the hydrogen bonded drive for β-hairpin formation is identical between diastereomers, the conformational differences we observe provide insight on the intrinsic folding propensities of the diastereomeric peptide or depsipeptide backbones. These intrinsic folding propensities are presumably determined by torsional strain and other nonbonded repulsions that develop as the peptide backbone folds back upon itself, and by conformational entropy.[19] (We assume that differences in solvation between diastereomers are energetically small, in all solvents.) Our results suggest that the correlation between mirror-image turns and two-residue loop β-hairpins observed in crystalline proteins[5] arises from competition between the intrinsically favored twist for two adjacent strands of β-sheet and the intrinsically favored backbone conformations for β-turns, with the former winning out.

The similarity of trends in the peptide and depsipeptide series validates our initial assumption that the depsipeptides are reasonable models for the conformational behavior of authentic peptide backbones. The β-hairpin fold appears to be modestly more stable in the heterochiral depsipeptides than in the analogous peptides, perhaps because of the equilibrium involving the γ-turn shown in Scheme 1, which is unique to the peptides.

2. A Common *β*-Turn Is an Impediment to Formation of a Two-Residue *β*-Hairpin Loop. This conclusion is based on the behavior of the all-L tetrapeptides and depsipeptides in methylene chloride, where failure to form a β-hairpin requires that the hydrogen bonding potential of Val N−H and Leu C=O remain unsatisfied. It is commonly assumed that stabilizing *any* β-turn necessarily promotes β-hairpin formation;[4a,b,20] however, our results show that the type of β-turn is crucial, and that the most common turn conformations for all-L peptides (types I and II) are antithetical to formation of a two-residue β-hairpin loop. The relationship between β-turn conformation and β-hairpin stabilization explains at least in part why several recently reported dipeptide-mimetic units that are locally achiral

(18) A recently described β-sheet protein design (ref 4d) includes the use of D-residues at positions intended to form two-residue β-hairpin loops.

(19) We recently reported that the β-hairpin conformation of four-residue depsipeptide Ac-Gly-Pro-Glyco-Gly-NMe_2 in CH_2Cl_2 is only about 40% populated at room temperature: Gardner, R. R.; Gellman, S. H. *J. Am. Chem. Soc.* **1995**, *117*, 10411. Comparison of this result with an observation reported here, complete population of β-hairpin for $^{D}V^{L}PGlyco^{D}L$, indicates that side chains, with the correct configuration, are required on the terminal residues for complete β-hairpin formation. These terminal residue side chains presumably decrease the number of non-hairpin conformations available to the backbone, thus decreasing the loss of conformational entropy associated with adoption of the hairpin folding pattern.

(20) Searle, M. S.; Williams, D. H.; Rackman, L. C. *Nature Struct. Biol.* **1995**, *2*, 999. For β-hairpin folding, in water, of a 16-residue peptide that lacks proline, see: Blanco, F. J.; Rivas, G.; Serrano, L. *Nature Struct. Biol.* **1994**, *1*, 584.

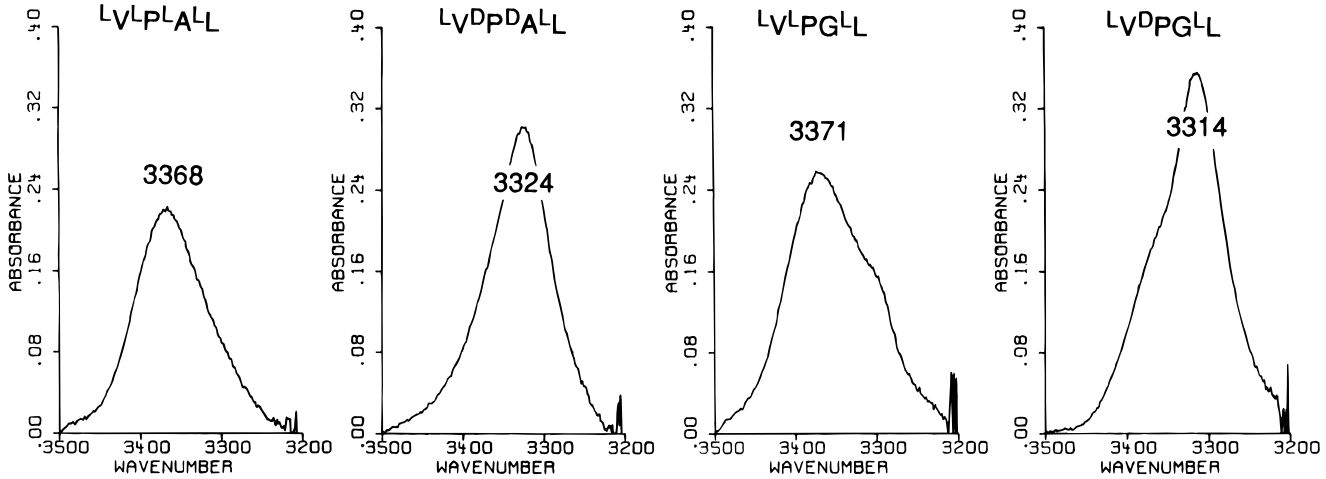

Figure 13. N−H stretch FT-IR data for 10 mM peptide samples in CH_3CN at room temperature, after subtraction of the spectrum of pure CH_3CN. From left to right: $^{L}V^{L}P^{L}A^{L}L$, maximum at 3368 cm^{-1}; $^{L}V^{D}P^{D}A^{L}L$, maximum at 3324 cm^{-1}; $^{L}V^{L}PG^{L}L$, maximum at 3371 and shoulder at 3303 cm^{-1}; $^{L}V^{D}PG^{L}L$, shoulder at 3371 cm^{-1} and maximum at 3314 cm^{-1}.

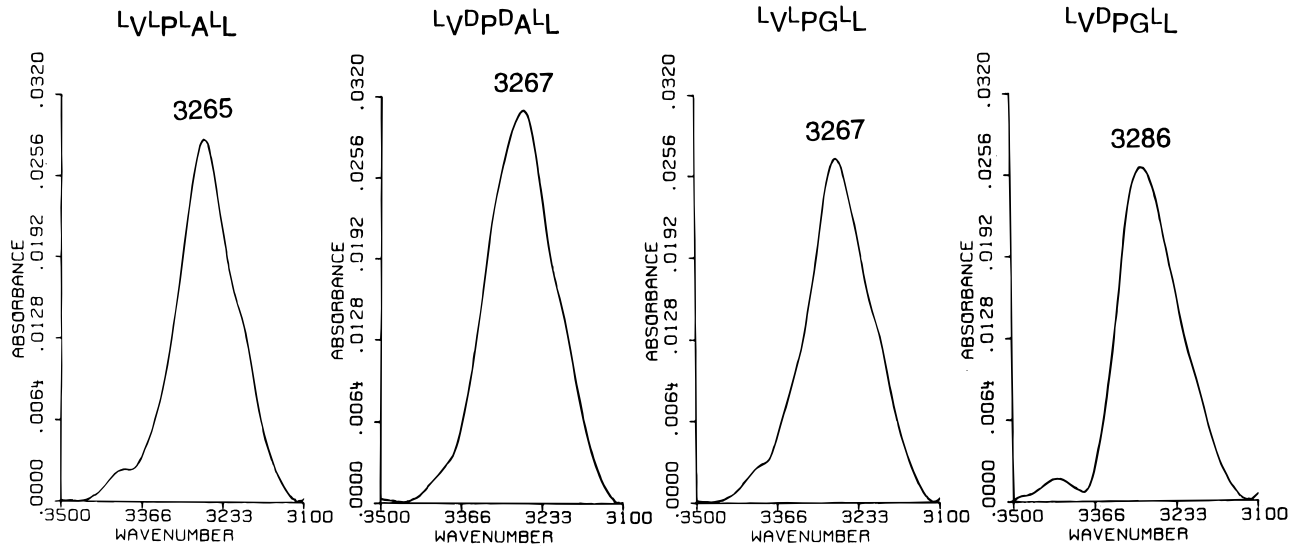

Figure 14. N−H stretch FT-IR data for 10 mM peptide samples in DMSO at room temperature, after subtraction of the spectrum of pure DMSO. From left to right: $^{L}V^{L}P^{L}A^{L}L$, maximum at 3265 cm^{-1}; $^{L}V^{D}P^{D}A^{L}L$, maximum at 3267 cm^{-1}; $^{L}V^{L}PG^{L}L$, maximum at 3265 cm^{-1}; $^{L}V^{D}PG^{L}L$, maximum at 3286 cm^{-1}.

strongly promote β-hairpin conformations in solution:[21] in the absence of a chiral center, the distinction between "common" and "mirror-image" turns disappears.

β-Hairpin conformations have recently been identified in two short all-L peptides (9 and 16 residues) in aqueous solution, both containing a proline residue in the turn region.[20,22] In both cases, the antiparallel β-strands are connected by a three-residue loop rather than a two-residue loop. We propose that the rigid L-proline residue in each of these peptides precludes a mirror-image turn, and therefore disfavors a two-residue β-hairpin loop. Consistent with this hypothesis, proline is rare in two-residue β-hairpin loops in crystalline proteins.[5b] Simple molecular mechanics comparison of $^{L}V^{L}P^{L}Lac^{L}L$ and $^{D}V^{L}P^{L}Lac^{D}L$ suggests that closure of the 14-membered hydrogen bonded ring requires greater internal steric repulsion in the all-L depsipeptide than in the heterochiral isomer, but full rationalization of our observations will require a more detailed analysis.

3. The Ability of Intramolecular Hydrogen Bonds To Induce Folding Is Limited, Even in Nonpolar Environments. The lack of significant β-hairpin formation among the all-L peptides and depsipeptides in methylene chloride indicates that closing the 14-membered-ring hydrogen bond costs more in terms of induced strain in the all-L backbones than would be gained by hydrogen bond formation. We have previously argued that chemists and biochemists tend to overemphasize the significance of hydrogen bonds in noncovalently controlled structure;[9a] the dramatic distinction in folding properties between the all-L molecules and their heterochiral isomers in methylene chloride is a good example of the perils of a hydrogen bond-centered view. It is difficult or impossible, upon visual inspection of drawings or physical models, to identify the features of the all-L backbones that oppose 14-membered-ring hydrogen bond formation of the four-residue molecules described here.

Experimental Section

Infrared Spectroscopy. Spectra were obtained on a Nicolet Model 740 FT-IR spectrometer. IR samples were prepared under anhydrous conditions; solvents were distilled from CaH_2 and stored over molecular

(21) (a) Díaz, H.; Tsang, K. Y.; Choo, D.; Espina, J. R.; Kelly, J. W. *J. Am. Chem. Soc.* **1993**, *115*, 3790. (b) Gardner, R. R.; Gellman, S. H. *J. Am. Chem. Soc.* **1995**, *117*, 10411. (c) Kemp, D. S.; Li, Z. Q. *Tetrahedron Lett.* **1995**, *36*, 4175, 4179.

(22) (a) Blanco, F. J.; Jiménez, M. A.; Herranz, J.; Rico, M.; Santoro, J.; Nieto, J. L. *J. Am. Chem. Soc.* **1993**, *115*, 5887. (b) Constantine, K. L.; Mueller, L.; Andersen, N. H.; Tong, H.; Wandler, C. F.; Friedrichs, M. S.; Bruccoleri, R. E. *J. Am. Chem. Soc.* **1995**, *117*, 10841. (c) Friedrichs, M. S.; Stouch, T. R.; Bruccoleri, R. E.; Mueller, L.; Constantine, K. L. *J. Am. Chem. Soc.* **1995**, *117*, 10855.

sieves, compounds and glassware were dried under vacuum overnight, and solutions were prepared under an N_2 atmosphere. The pure solvent spectrum for a particular solution was subtracted from the sample spectrum prior to analysis. Peaks in the amide NH stretch region were baseline corrected, and analyzed without further manipulation.

NMR Spectroscopy. 1. Aggregation Studies. One-dimensional spectra for aggregation studies were obtained on either a Varian Unity-500 or a Bruker AM-500 spectrometer. Samples for aggregation studies were prepared by serial dilution from the most concentrated sample (typically 40 to 50 mM). Dry compounds were dissolved in CD_2Cl_2 previously dried over 3 Å molecular sieves, and samples were prepared with dry glassware under an N_2 atmosphere.

2. Conformational Analysis. NMR samples for conformational analysis were prepared by dissolving the dry compound in dry deuterated solvent under an N_2 atmosphere. Samples were then degassed by the freeze−pump−thaw method, and the NMR tubes were sealed under vacuum. All two-dimensional NMR spectra were obtained on a Varian Unity-500 spectrometer. Proton signals were assigned via TOCSY[23] spectra, and ROESY[12] or NOESY[17] spectra provided the data used in the conformational analyses. Two-dimensional spectra were acquired using standard Varian pulse sequences and hypercomplex phase cycling (States-Haberkorn method[24]), and the data were processed with Varian VNMR version 4.3 software. TOCSY spectra were recorded with 2048 points in t_1, 256 or 512 points in t_2, and either 8 or 16 scans per t_2 increment. ROESY and NOESY spectra were recorded with a similar number of t_1 and t_2 points unless otherwise noted, and between 32 and 120 scans per t_2 increment, depending on the concentration of the sample. The width of the spectral window examined was between 4500 and 6000 Hz. Sample concentrations for two-dimensional spectra were 1 mM in CD_2Cl_2, 5 or 10 mM in CD_3CN, and 10 mM in DMSO-d_6.

3. NOESY Buildup Plots: NOESY spectra were obtained for five different mixing times (ranging from 250 to 1250 ms) for each buildup curve. Intensities were normalized between spectra in the following manner. For the observed NOE interaction at a particular mixing time, the volume integrations of the two cross peaks were averaged. The average NOE volume was then divided by the average of the volume integrations of the two corresponding diagonal peaks. The resulting normalized NOE intensity was multiplied by an arbitrary number (in the cases discussed here, 1000). Normalized NOEs for a specific interaction were then plotted as a function of mixing time to obtain a buildup plot.

X-ray Crystallography. Crystals suitable for X-ray analysis were obtained by vapor diffusion (over several days) of hexane into a solution of the particular depsipeptide in ethyl acetate. In several cases it was necessary to use dried solvents and grow the crystals under anhydrous conditions.

Synthesis. Depsipeptides and peptides were synthesized by standard dicyclohexylcarbodiimide/*N*-hydroxysuccinimide (DCC/HOSu) solution-phase coupling procedures.[25] Representative procedures are given below.

Formation of Activated Ester Boc-L-Ala-OSu. Boc-L-Ala-OH (0.150 g, 0.791 mmol) was dissolved in 5 mL of CH_2Cl_2. HOSu (0.091 g, 0.791 mmol) was then added to the solution, followed by 0.163 g of DCC (0.791 mmol). Several minutes after DCC addition, the formation of a white precipitate was observed. The solution was stirred at room temperature for 1 h. The crude activated ester was then allowed to react with the selected nucleophile.

Peptide Deprotection and Coupling Procedure. Boc-L-Ala-L-Leu-NMe_2: Boc-L-Leu-NMe_2 (0.170 g, 0.659 mmol) was dissolved in 2 mL of 4 N HCl/dioxane, and the solution was stirred at room temperature for 1 h. The remaining HCl/dioxane was then removed by bubbling N_2 through the solution. CH_2Cl_2 (2−3 mL) was added to the resulting solid, followed by 0.110 mL of triethylamine (0.791 mmol). The resulting solution was added to the solution containing the activated ester Boc-L-Ala-OSu, and the combined reaction solution was stirred overnight (10−12 h). The white solid was filtered off, and the remaining solution was concentrated to yield a white solid. The solid was purified by silica gel chromatography (eluting with 50:49:1 ethyl acetate/chloroform/methanol) to yield 0.125 g (0.381 mmol, 58%) of the desired dipeptide as a white solid.

α-Hydroxy Acid Coupling. HO-L-Lac-D-Leu-NMe_2: Boc-D-Leu-NMe_2 (0.500 g, 1.94 mmol) was deprotected as described above. The activated ester was prepared by addition of 0.253 g of HOSu (2.20 mmol) followed by 0.453 g of DCC (2.20 mmol) to a CH_2Cl_2 solution of L-lactic acid (0.192 g, 2.14 mmol). A white precipitate formed soon after DCC addition. The solution of H_2N-D-Leu-NMe_2 and triethylamine in CH_2Cl_2 was then transferred into the activated ester solution. After stirring the resulting solution overnight, the white solid was filtered off, and the remaining solution was concentrated to a clear colorless oil. Purification by silica gel chromatography (eluting with 4% MeOH in $CHCl_3$) yielded 0.381 g of the desired product as a clear colorless oil (1.66 mmol, 86%).

HO-D-Lac-D-Leu-NMe_2: A modified coupling procedure was used in obtaining this product, since D-lactic acid was purchased as the lithium salt, which is insoluble in CH_2Cl_2. The coupling reaction was run in 3:2 DMF/CH_2Cl_2. The desired product was obtained in a yield of 67% after silica gel chromatography.

Ester Bond Formation. Boc-L-Pro-D-Lac-L-Leu-NMe_2: HO-D-Lac-L-Leu-NMe_2 (0.130 g, 0.565 mmol) was dissolved in 20 mL of CH_2Cl_2, followed by 0.133 g of Boc-L-Pro-OH (0.620 mmol). The resulting clear solution was cooled to 0 °C. 4-(Dimethylamino)pyridine (0.009 g, 0.074 mmol) was added, followed by 0.128 g of DCC (0.620 mmol), and the solution was stirred at 0 °C for 1 h, then allowed to warm to room temperature and stirred for another 4 h. The solution turned cloudy 25 min after DCC addition. The precipitate was filtered off, and the solution was concentrated under vacuum. The resulting solid was purified by silica gel chromatography (eluting with ethyl acetate) to afford 0.158 g of the product as a white solid (0.370 mmol, 65%).

Capping Procedure. Ac-D-Val-L-Pro-L-Lac-D-Leu-NMe_2: Tetrapeptide Boc-D-Val-L-Pro-L-Lac-D-Leu-NMe_2 was deprotected with 4 N HCl/dioxane as described above. Triethylamine (0.16 mL, 1.14 mmol) was added to the solid, and the mixture was dissolved in 5 mL of CH_2Cl_2. The solution was cooled to 0 °C, and 0.047 mL of acetic anhydride (0.500 mmol) was added to the stirring solution. The solution was stirred at 0 °C for 1 h, then allowed to warm to room temperature and stirred another 2 h. The organic solution was washed with 20 mL of 10% HCl (aq), then 2 × 20 mL of 5% $NaHCO_3$ (aq), and dried with $MgSO_4$. The solution was filtered and concentrated under vacuum. The resulting crude solid was purified by silica gel chromatography (eluting with 4% MeOH in $CHCl_3$) to yield 0.152 g of the final product as a white solid (0.325 mmol, 86%). Running the capping reaction in methanol or with acetyl chloride instead of acetic anhydride resulted in a reduced yield of the final product.

Characterization. Final compounds were characterized by ^{1}H and ^{13}C NMR, FTIR, and high-resolution mass spectroscopy. NMR spectra are referenced to the solvent peak of the sample. ^{13}C spectra were acquired with ^{1}H decoupling, and all ^{13}C peaks reported are one-carbon singlets when ^{1}H decoupled, unless otherwise noted. ^{1}H and ^{13}C NMR spectra reported for characterization were obtained on purified samples on a Varian Unity-500 NMR spectrometer or a Bruker AC-300 or AM-500 NMR spectrometer. Ester C═O stretch and amide I IR bands observed for solutions of compounds in methylene chloride are listed, where "(sh)" indicates that the peak is a shoulder on an adjacent peak. All final compounds were very pure, as no impurities were detectable via ^{1}H or ^{13}C NMR spectroscopy.

Ac-^{L}V^{L}P^{L}Lac^{L}L-NMe_2: ^{1}H NMR (CD_2Cl_2, 500 MHz) δ 0.92 (d, J = 6.6 Hz, 3 H), 0.93 (d, J = 6.9 Hz, 3 H), 0.97 (d, J = 6.4 Hz, 3 H), 1.00 (d, J = 6.7 Hz, 3 H), 1.44 (d, J = 7.0 Hz, 3 H), 1.51 (m, 4 H), 1.98 (s, 3 H), 2.07 (m, 3 H), 2.29 (m, 1 H), 2.90 (s, 3 H), 3.02 (s, 3 H), 3.65 (m, 1 H), 3.82 (m, 1 H), 4.49 (dd, J = 8.4, 6.1 Hz, 1 H), 4.63 (dd, J = 9.0, 6.7 Hz, 1 H), 4.87 (td, J = 8.6, 5.0 Hz, 1 H), 5.09 (q, J = 7.0 Hz, 1 H), 6.27 (d, J = 8.7 Hz, 1 H), 7.13 (d, J = 7.3 Hz, 1 H). ^{13}C NMR (CD_2Cl_2, 125.8 MHz) δ 15.27, 17.96, 18.06, 18.16, 19.33, 22.08, 23.24, 23.38, 24.92, 25.38, 29.35, 31.02, 35.84, 37.17, 42.32, 47.89, 59.65, 71.56, 169.98, 170.12, 170.85, 171.89, 171.95. FTIR ν (cm^{-1}) 1754 (sh), 1744, 1674, 1644, 1632 (sh), 1509. EI-MS m/z (M^+) calculated for $C_{23}H_{40}N_4O_6$ 468.2948, observed 468.2960.

Ac-^{D}V^{L}P^{L}Lac^{D}L-NMe_2: ^{1}H NMR (CD_2Cl_2, 500 MHz) δ 0.92 (d, J = 6.6 Hz, 6 H), 0.93 (d, J = 4.9 Hz, 3 H), 0.96 (d, J = 6.8 Hz, 3 H),

(23) Braunschweiler, L.; Ernst, R. R. *J. Magn. Reson.* **1983**, *53*, 521.
(24) States, D. J.; Haberkorn, R. A.; Ruben, D. J. *J. Magn. Reson.* **1982**, *48*, 286.
(25) Bodanszky, M.; Bodanszky, A. *The Practice of Peptide Synthesis*; Springer-Verlag: New York, 1984.

1.32 (d, J = 7.1 Hz, 3 H), 1.34 (m, 1 H), 1.88 (ddd, J = 13.8, 11.1, 4.3 Hz, 1 H), 1.92 (s, 3 H), 2.00 (m, 4 H), 2.27 (m, 1 H), 2.93 (s, 3 H), 3.13 (s, 3 H), 3.68 (dt, J = 10.3, 6.9 Hz, 1 H), 4.04 (dt, J = 10.2, 6.6 Hz, 1 H), 4.46 (dd, J = 8.9, 4.4 Hz, 1 H), 4.61 (t, J = 9.9 Hz, 1 H), 4.95 (ddd, J = 11.1, 8.5, 3.8 Hz, 1 H), 5.16 (q, J = 7.1 Hz, 1 H), 7.64 (d, J = 8.5 Hz, 1 H), 8.40 (d, J = 9.8 Hz, 1 H). ^{13}C NMR (CD_2Cl_2, 125.8 MHz) δ 18.10, 18.63, 19.37, 21.56, 22.54, 23.44, 24.98, 25.30, 29.71, 30.93, 35.89, 37.34, 40.67, 47.44, 47.94, 56.34, 59.99, 70.68, 170.08, 170.45, 170.91, 172.70, 173.45. FTIR ν (cm^{-1}) 1743, 1666, 1644 (sh) 1629, 1539. EI-MS m/z (M^+) calculated for $C_{23}H_{40}N_4O_6$ 468.2948, observed 468.2960.

Ac-^{D}V^{L}P^{D}Lac^{D}L-NMe$_2$: ^{1}H NMR (CD_2Cl_2, 500 MHz) δ 0.92 (d, J = 6.6 Hz, 6 H), 0.93 (d, J = 6.9 Hz, 3 H), 0.94 (d, J = 6.7 Hz, 3 H), 1.48 (d, J = 7.2 Hz, 3 H), 1.51 (m, 1 H), 1.67 (p, J = 6.4 Hz, 1 H), 1.85 (ddd, J = 13.9, 9.5, 4.7 Hz, 1 H), 2.01 (m, 2 H), 2.04 (s, 3 H), 2.15 (m, 3 H), 2.89 (s, 3 H), 3.18 (s, 3 H), 3.63 (td, J = 8.5, 5.8 Hz, 1 H), 3.79 (td, J = 7.9, 5.9 Hz, 1 H), 4.41 (dd, J = 7.9, 4.4 Hz, 1 H), 4.57 (t, J = 9.0 Hz, 1 H), 4.90 (td, J = 9.2, 5.2 Hz, 1 H), 5.07 (q, J = 7.0 Hz, 1 H), 7.82 (d, J = 9.5 Hz, 1 H), 8.04 (d, J = 8.6 Hz, 1 H). ^{13}C NMR ($CDCl_3$, 75.4 MHz) δ 17.40, 18.07, 18.84, 21.81, 22.45, 22.73, 24.37, 24.95, 28.37, 30.88, 35.71, 37.08, 40.26, 46.46, 47.07, 55.54, 58.80, 70.76, 169.84, 170.49, 170.86, 171.99 (2 C). FTIR ν (cm^{-1}) 1749, 1665, 1641 (sh), 1630, 1538. (EI-MS m/z (M^+) calculated for $C_{23}H_{40}N_4O_6$ 468.2948, observed 468.2949.

Ac-^{L}V^{L}PGlyco^{L}L-NMe$_2$: ^{1}H NMR (CD_2Cl_2, 500 MHz) δ 0.89 (d, J = 6.7 Hz, 3 H), 0.91 (d, J = 6.4 Hz, 3 H), 0.95 (d, J = 6.4 Hz, 3 H), 0.97 (d, J = 6.7 Hz, 3 H), 1.52 (m, 2 H), 1.58 (m, 1 H), 1.99 (s, 3 H), 2.05 (m, 2 H), 2.10 (m, 2 H), 2.29 (m, 1 H), 2.91 (s, 3 H), 3.05 (s, 3 H), 3.67 (m, 1 H), 3.85 (m, 1 H), 4.43 (t, J = 7.6 Hz, 1 H), 4.44 (d, J = 15.4 Hz, 1 H), 4.63 (dd, J = 9.0, 6.6 Hz, 1 H), 4.73 (d, J = 15.4 Hz, 1 H), 4.96 (dd, J = 15.6, 7.0 Hz, 1 H), 6.35 (d, J = 8.2 Hz, 1 H), 7.40 (d, J = 8.2 Hz, 1 H). ^{13}C NMR (CD_2Cl_2) δ 17.78, 18.92, 21.99, 22.86, 24.38, 25.06, 28.90, 29.47, 31.33, 35.58, 36.93, 42.02, 46.74, 47.37, 55.29, 59.07, 62.35, 166.38, 170.08, 171.02, 171.28, 171.72. FTIR ν (cm^{-1}) 1757, 1673, 1644, 1633, 1508. EI-MS m/z (M^+) calculated for $C_{22}H_{38}N_4O_6$ 454.2791, observed 454.2782.

Ac-^{D}V^{L}PGlyco^{D}L-NMe$_2$: ^{1}H NMR (CD_2Cl_2, 500 MHz) δ 0.92 (d, J = 6.7 Hz, 6 H), 0.94 (d, J = 7.2 Hz, 3 H), 0.96 (d, J = 6.7 Hz, 3 H), 1.42 (ddd, J = 13.6, 9.3, 4.2 Hz, 1 H), 1.66 (m, 1 H), 1.86 (ddd, J = 13.9, 10.7, 4.6 Hz, 1 H), 1.95 (s, 3 H), 2.02 (m, 4 H), 2.26 (m, 1 H), 2.92 (s, 3 H), 3.15 (s, 3 H), 3.68 (dt, J = 10.5, 6.6 Hz, 1 H), 3.99 (dt, J = 10.6, 6.2 Hz, 1 H), 4.21 (d, J = 15.6 Hz, 1 H), 4.46 (dd, J = 8.4, 4.4 Hz, 1 H), 4.61 (t, J = 9.6 Hz, 1 H), 4.90 (d, J = 15.4 Hz, 1 H), 5.00 (ddd, J = 10.7, 8.6, 4.2 Hz, 1 H), 7.83 (d, J = 8.6 Hz, 1 H), 8.25 (d, J = 9.2 Hz, 1 H). ^{13}C NMR ($CDCl_3$, 125.7 MHz) δ 18.51, 19.23, 21.75, 22.43, 23.19, 24.72, 25.08, 29.14, 30.63, 35.84, 37.24, 40.56, 47.04, 47.66, 56.13, 59.56, 62.67, 166.96, 170.89, 172.29, 173.01, 173.49. FTIR ν (cm^{-1}) 1753, 1666, 1641 (sh), 1628, 1543. EI-MS m/z (M^+) calculated for $C_{22}H_{38}N_4O_6$ 454.2791, observed 454.2804.

Ac-^{L}V^{L}P^{L}A^{L}L-NMe$_2$: ^{1}H NMR (CD_2Cl_2, 500 MHz) δ 0.90 (d, J = 6.7 Hz, 3 H), 0.91 (d, J = 6.9 Hz, 3 H), 0.97 (d, J = 6.9 Hz, 3 H), 0.97 (d, J = 6.4 Hz, 3 H), 1.28 (d, J = 7.2 Hz, 3 H), 1.43 (m, 3 H), 1.59 (m, 1 H), 1.97 (s, 3 H), 2.04 (m, 2 H), 2.26 (m, 1 H), 2.90 (s, 3 H), 3.04 (s, 3 H), 3.60 (m, 1 H), 3.74 (m, 1 H), 4.33 (p, J = 7.2 Hz, 1 H), 4.51 (dd, J = 8.0, 3.9 Hz, 1 H), 4.61 (dd, J = 8.9, 6.3 Hz, 1 H), 4.89 (td, J = 9.1, 3.8 Hz, 1 H), 6.17 (d, J = 9.5 Hz, 1 H), 6.71 (d, J = 8.4 Hz, 1 H), 7.13 (d, J = 7.3 Hz, 1 H). ^{13}C NMR ($CDCl_3$, 125.7 MHz) δ 17.93, 18.23, 19.27, 21.97, 22.96, 23.33, 24.70, 25.14, 27.93, 31.44, 35.74, 37.00, 42.37, 47.34, 47.80, 49.02, 55.68, 60.04, 170.08, 171.03, 171.76, 172.03, 172.24. FTIR ν (cm^{-1}) 1675, 1645, 1627 (sh), 1504. HR-LSIMS; calculated for $C_{23}H_{41}N_5O_5 + H^+$ 468.3186, observed 468.3189.

Ac-^{L}V^{D}P^{D}A^{L}L-NMe$_2$: ^{1}H NMR (CD_2Cl_2, 500 MHz) δ 0.90 (d, J = 6.4 Hz, 3 H), 0.91 (d, J = 6.1 Hz, 3 H), 0.96 (d, J = 6.7 Hz, 3 H), 1.03 (d, J = 6.7 Hz, 3 H), 1.30 (d, J = 7.6 Hz, 3 H), 1.39 (ddd, J = 13.6, 9.2, 4.3 Hz, 1 H), 1.63 (m, 1 H), 1.80 (ddd, J = 14.0, 9.9, 4.4 Hz, 1 H), 1.92 (s, 3 H), 2.01 (m, 3 H), 2.07 (m, 1 H), 2.25 (m, 1 H), 2.91 (s, 3 H), 3.14 (s, 3 H), 3.64 (m, 1 H), 4.20 (m, 1 H), 4.26 (t, J = 8.7 Hz, 1 H), 4.34 (p, J = 7.0 Hz, 1 H), 4.38 (dd, J = 8.6, 4.0 Hz, 1 H), 4.86 (m, 1 H), 6.32 (d, J = 7.9 Hz, 1 H), 7.26 (d, J = 7.6 Hz, 1 H), 7.56 (d, J = 6.4 Hz, 1 H). ^{13}C NMR (CD_2Cl_2, 125.8 MHz) δ 17.71, 19.04, 19.30, 21.85, 22.76, 23.41, 24.95, 25.28, 29.76, 30.29, 35.89, 37.43, 40.95, 47.78, 48.09, 48.97, 58.03, 61.84, 171.25, 172.13, 172.71, 172.82, 173.19. FTIR ν (cm^{-1}) 1680 (sh), 1656, 1635, 1533, 1507. HR-LSIMS; calculated for $C_{23}H_{41}N_5O_5 + H^+$ 468.3186, observed 468.3186.

Ac-^{D}V^{L}P(^{15}N)^{L}A^{D}L-NMe$_2$: ^{1}H NMR (CD_2Cl_2, 300 MHz) δ 0.89 (d, J = 6.3 Hz, 3 H), 0.90 (d, J = 6.3 Hz, 3 H), 0.94 (d, J = 6.6 Hz, 3 H), 1.02 (d, J = 7.0 Hz, 3 H), 1.32 (dd, J = 7.4, 2.9 Hz, 3 H), 1.41 (ddd, J = 13.8, 9.0, 4.8, Hz, 1 H), 1.65 (m, 1 H), 1.86 (m, 1 H), 1.92 (s, 3 H), 2.01 (m, 4 H), 2.26 (m, 1 H), 2.91 (s, 3 H), 3.17 (s, 3 H), 3.62 (dt, J = 10.1, 7.0 Hz, 1 H), 4.28 (m, 2 H), 4.43 (m, 2 H), 4.87 (ddd, J = 10.3, 8.1, 4.4 Hz, 1 H), 6.15 (dd, J = 90.8, 8.8 Hz, 1 H), 7.42 (d, J = 7.7 Hz, 1 H), 7.81 (d, J = 8.5 Hz, 1 H). ^{13}C NMR ($CDCl_3$, 75.4 MHz) δ 17.35, 18.72, 19.02, 21.57, 22.36, 23.05, 24.38, 24.74, 29.14, 29.49, 35.62, 37.09, 40.33, 47.45, 47.51, 48.11 (d, ^{15}N−^{13}C J = 17 Hz), 57.55, 61.20 (d, ^{15}N−^{13}C J = 12 Hz), 170.70 (d, ^{15}N−^{13}C J = 25 Hz), 171.80, 172.30, 172.61, 172.96. FTIR ν (cm^{-1}) 1680 (sh), 1656, 1635, 1530. HR-LSIMS; calculated for $C_{23}H_{41}{}^{15}NN_4O_5 + H^+$ 469.3156, observed 469.3143.

Ac-^{L}V^{L}PG^{L}L-NMe$_2$: ^{1}H NMR (CD_2Cl_2, 500 MHz) δ 0.88 (d, J = 6.9 Hz, 3 H), 0.90 (d, J = 6.6 Hz, 3 H), 0.95 (d, J = 6.6 Hz, 3 H), 0.96 (d, J = 6.7 Hz, 3 H), 1.47 (m, 2 H), 1.59 (m, 1 H), 1.96 (m, 1 H), 1.99 (s, 3 H), 2.06 (m, 3 H), 2.19 (m, 1 H), 2.91 (s, 3 H), 3.06 (s, 3 H), 3.62 (m, 1 H), 3.71 (dd, J = 16.9, 4.9 Hz, 1 H), 3.78 (m, 1 H), 4.05 (dd, J = 16.9, 6.9 Hz, 1 H), 4.36 (t, J = 6.5 Hz, 1 H), 4.63 (dd, J = 9.0, 6.4 Hz, 1 H), 4.94 (dt, J = 8.6, 5.6 Hz, 1 H), 6.35 (d, J = 9.0 Hz, 1 H), 6.79 (bt, 1 H), 7.03 (d, J = 7.2 Hz, 1 H). ^{13}C NMR ($CDCl_3$, 125.8 MHz) δ 17.87, 19.34, 22.05, 22.95, 23.14, 24.65, 25.14, 28.43, 31.29, 35.75, 37.06, 42.09, 42.99, 47.31, 47.79, 55.68, 60.51, 168.43, 170.10, 171.76, 171.87, 172.24. FTIR ν (cm^{-1}) 1694, 1673, 1645, 1630, 1534, 1507. EI-MS m/z (M^+) calculated for $C_{22}H_{39}N_5O_5$ 453.2951, observed 453.2958.

Ac-^{L}V^{D}PG^{L}L-NMe$_2$: ^{1}H NMR (CD_2Cl_2, 500 MHz) δ 0.91 (d, J = 6.6 Hz, 3 H), 0.92 (d, J = 6.6 Hz, 3 H), 0.95 (d, J = 6.6 Hz, 3 H), 1.00 (d, J = 6.9 Hz, 3 H), 1.43 (ddd, J = 13.7, 8.9, 4.6 Hz, 1 H), 1.64 (m, 1 H), 1.78 (ddd, J = 14.0, 9.8, 4.5 Hz, 1 H), 1.94 (s, 3 H), 2.04 (m, 4 H), 2.21 (m, 1 H), 2.97 (s, 3 H), 3.15 (s, 3 H), 3.57 (dd, J = 17.3, 5.7 Hz, 1 H), 3.63 (m, 1 H), 4.02 (dd, J = 17.4, 7.3 Hz, 1 H), 4.08 (m, 1 H), 4.35 (m, 1 H), 4.93 (ddd, J = 10.2, 8.4, 4.5 Hz, 1 H), 6.56 (bt, J = 6.0 Hz, 1 H), 7.45 (d, J = 8.2 Hz, 1 H), 7.72 (d, J = 8.4 Hz, 1 H). ^{13}C NMR (CD_2Cl_2, 125.8 MHz) δ 18.94, 19.34, 21.89, 22.63, 23.39, 24.94, 25.26, 29.66, 31.01, 35.98, 37.49, 41.13, 42.90, 47.39, 48.13, 57.61, 61.79, 168.99, 172.00, 172.40, 172.52, 173.20. FTIR ν (cm^{-1}) 1690, 1659, 1632, 1538, 1518. EI-MS m/z (M^+) calculated for $C_{22}H_{39}N_5O_5 + H^+$ 454,3029, observed 454.3021.

Acknowledgment. This work was supported in part by the Army Research Office and by the National Science Foundation. T.S.H. was the recipient of a National Research Service Award (T32 GM08923). The authors thank Dr. Doug Powell and Mr. Kurt Schladetzky for their assistance in obtaining the crystallographic data.

Supporting Information Available: Representative ROESY and NOESY spectra for several compounds and structure factor sets for the four crystal structures (45 pages). See any current masthead page for ordering and Internet access instructions.

JA960429J